AIP | Applied Physics Letters

Identification of photo-induced spin-triplet recombination centers situated at Si surfaces and Si/SiO2 interfaces

M. Otsuka, T. Matsuoka, L. S. Vlasenko, M. P. Vlasenko, and K. M. Itoh

Citation: Appl. Phys. Lett. **103**, 111601 (2013); doi: 10.1063/1.4820824
View online: http://dx.doi.org/10.1063/1.4820824
View Table of Contents: http://apl.aip.org/resource/1/APPLAB/v103/i11
Published by the AIP Publishing LLC.

Identification of photo-induced spin-triplet recombination centers situated at Si surfaces and Si/SiO_2 interfaces

M. Otsuka,[1] T. Matsuoka,[1] L. S. Vlasenko,[2] M. P. Vlasenko,[2] and K. M. Itoh[1]
[1]*School of Fundamental Science and Technology, Keio University, 3-14-1 Hiyoshi, Kohoku-ku, Yokohama 223-8522, Japan*
[2]*A. F. Ioffe Physico-Technical Institute, Russian Academy of Sciences, 194021 St. Petersburg, Russia*

(Received 18 June 2013; accepted 26 August 2013; published online 10 September 2013)

A recombination center at Si surfaces and Si/SiO_2 interfaces was identified using highly sensitive spin-dependent recombination (SDR) detection of electron paramagnetic resonance (EPR). The defect (Si-KU1) has a spin-triplet ($S = 1$) state owing to excitation by band-edge light employed in measurement. The Si-KU1 SDR-EPR spectrum exhibits orthorhombic symmetry along two equivalent $\langle 110 \rangle$ axes running parallel to the interface, which disappears upon mechanical lapping of the surface oxide or heat treatment above 400 °C. However, removal of surface oxide with diluted HF solution sharpens the Si-KU1 SDR-EPR lines. A plausible structural model of the center responsible for Si-KU1 is presented. © *2013 AIP Publishing LLC*. [http://dx.doi.org/10.1063/1.4820824]

Defects on silicon surfaces and at interfaces between silicon and silicon dioxide have been studied extensively in the past 40 years because they can strongly affect the device performance of the metal–oxide–silicon field-effect transistor.[1] The most well-known defects found by electron paramagnetic resonance (EPR) of the Si/SiO_2 interface are dangling bond defects (P_b centers)[2] that can be classified as P_b for (111) and (110) interfaces, and P_{b0} and P_{b1} for (100) interfaces.[3–6] Such defects very often act as recombination centers, and they are therefore observable using a special EPR technique using highly sensitive spin-dependent-recombination (SDR) detection.[7–13] Such a SDR-EPR detection scheme has sensitivity that is a few orders of magnitude higher than that of the conventional EPR method.[7–13] Applying the SDR-EPR detection scheme, photo-excited spin-triplet ($S = 1$) defects in irradiated silicon[11,12] and paramagnetic defects at the Si/SiO_2 interface (P_m centers)[13] were discovered recently. The concentrations of such defects are typically much lower than the detection limit of conventional EPR spectroscopy.

The present work reports identification of a previously unreported defect at Si surfaces and Si/SiO_2 interfaces using SDR-EPR. This defect, hereafter referred to as Si-KU1, was generated by band-edge light illumination and possessed spin-triplet excited states ($S = 1$). The samples employed were a commercially available n-type phosphorus-doped Czochralski (Cz)-grown (100) wafer $\rho \sim 5\,\Omega$ cm, and a highly resistive float-zone (FZ)-grown (100) wafer with $\rho > 2500\,\Omega$ cm. The SDR-EPR measurements were performed using an X-band EPR spectrometer (JEOL JES-RE3X) with a cylindrical TE_{011}-mode cavity and an externally applied magnetic field modulated by a frequency of 100 kHz. Under saturation of the target EPR transition using microwave power of 100–200 mW, the SDR-EPR signals were measured as a change in the microwave photoconductivity of the sample induced by a 100-W halogen lamp. No electrical contact with the sample was needed because the change in the photoconductivity was monitored as the change in the microwave absorption by photo-excited carriers of the sample in the cavity. The temperature of the samples was varied in the range of 4–80 K using an Oxford Instruments ESR900 helium-gas-flow cryostat. Because the lifetime of the photo-excited carriers is limited typically by the electron–hole recombination rate at such low temperatures, the concentration of the photo-excited carriers (i.e., the sample photoconductivity) changes upon EPR of recombination centers that can either lift or install the spin blockade against carrier recombination. Therefore, EPR of target recombination centers affects the sample photoconductivity, which can be detected as a change in the cavity quality (Q) factor in measurements of microwave reflectivity. A broad background due to the change in the sample magnetoresistance was suppressed by recording the second derivative of the EPR lines. The angular dependences of the EPR line positions were measured under rotation of the sample around the $\langle 110 \rangle$ axis placed perpendicular to the externally applied magnetic field. The line positions in units of the magnetic field were determined accurately using well-established phosphorus EPR line positions or Si-SL1 EPR line positions of the excited triplet state of the oxygen + vacancy center[14] appearing in the same spectrum as a reference. The majority of the measurements was performed for the interface between silicon and silicon dioxide formed naturally in air; i.e., native oxide. Furthermore, the effect of the removal of the oxide by mechanical lapping or dipping in 2.5% HF solution was investigated.

Initially, conventional EPR measurements were performed but, as expected from the limited sensitivity of such measurements, no signal originating from the surface or interface centers was detected. Only phosphorus EPR lines were observed with the Cz Si sample. Using the highly sensitive SDR-EPR approach, however, new SDR-EPR peaks were found as follows. The upper line of Figure 1 shows SDR-EPR spectra observed with the highly resistive (100)-oriented FZ Si sample having naturally formed SiO_2 (native oxide) on the surfaces. The spectrum consists of four lines labeled Si-KU1 and a central line at ~323 mT that is composed of many EPR lines that are grouped together and arise from spin $S = 1/2$ surface recombination centers P_{b0}, P_{b1}, P_m,

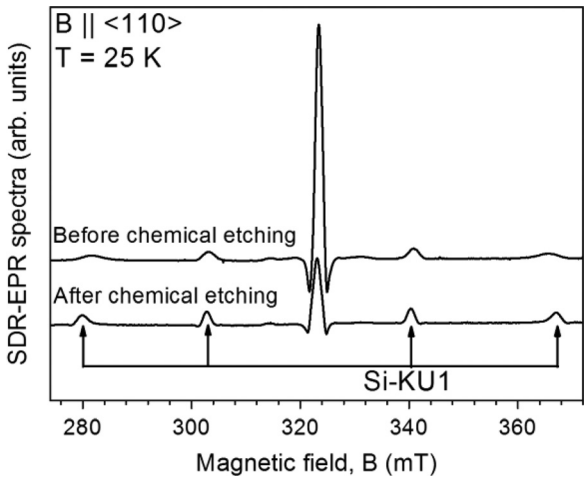

FIG. 1. SDR-EPR spectra for (100) FZ-grown silicon wafer having native oxide on the surface. The two spectra correspond to before and after etching of the same sample in a solution having a HNO_3:HF ratio of 3:1. The weak satellites observed near each line especially after etching originate most likely from the hyperfine interaction with nearby ^{29}Si nuclear spins.

E′, and their ^{29}Si hyperfine splitting lines.[4] Note that the central line with this intensity typically leads to a fractional change of 10^{-5} in the photocurrent when using the electrically detected magnetic resonance with two electrical contacts.[15] From the observation in Fig. 1 that the intensity (or the integrated area) of KU1 is about one order of magnitude less than that of the central line, we expect the fractional change in the photocurrent between KU1 in and out of resonance is about 10^{-6}. Similar spectra were observed for the Cz Si samples. The maximum intensity of the Si-KU1 peaks was obtained at sample temperatures of 25–40 K using the FZ Si sample. Detection of similar spectra in lower-resistance samples required lower temperatures of 15–20 K. The Si-KU1 peak intensities were 10–20 times weaker for the (111) Si wafers. The lower line of Figure 1 shows a spectrum taken with the same sample after chemical etching of the surface with a solution having a HNO_3:HF ratio of 3:1. Here, the Si-KU1 peaks did not disappear and their intensities grew and linewidths sharpened. It is well known

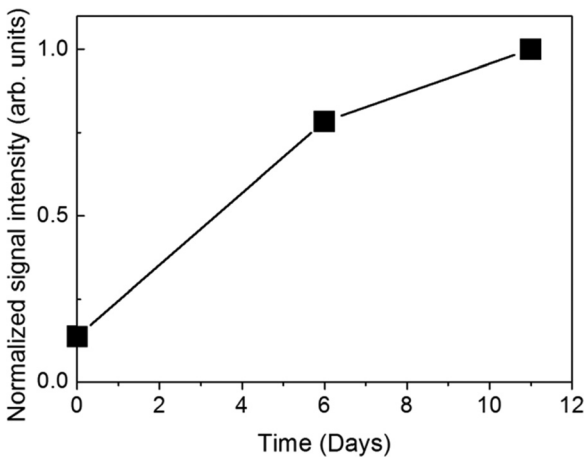

FIG. 2. Relative intensity of the Si-KU1 peak at 310 mT as a function of time (days) after the removal of the surface oxide. The sample was left in air at room temperature after the removal. Here, the intensity is normalized to that before the removal of the oxide; i.e., to that before etching in Fig. 1. It is seen that the full intensity is retrieved in ∼10 days.

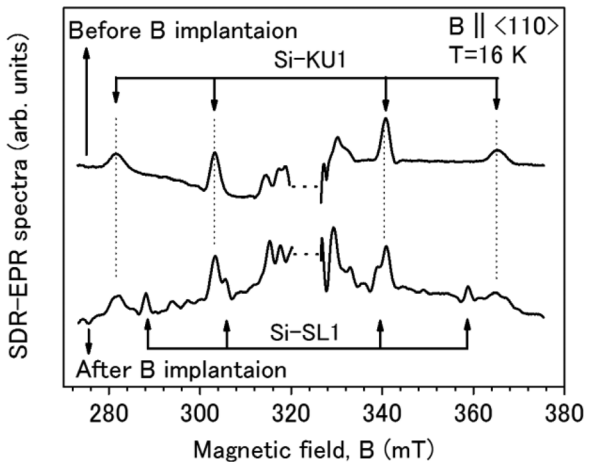

FIG. 3. SDR-EPR spectra observed with a Cz-grown (100)-Si wafer before and after 30-keV boron ion implantation with a dose of 10^{10} cm^{-2}.

that etching with an HNO_3:HF ratio of 3:1 leaves a newly formed oxide layer at the surface. Therefore, the defects related to Si-KU1 peaks were formed at the new interface with further suppression of causes (e.g., strain) leading to inhomogeneous broadening of the peaks. Figure 2 shows the time evolution of the SDR-EPR spectra after removal of the surface oxide with diluted HF. Here, it was rather surprising that the Si-KU1 peaks did not disappear and, immediately after the removal of the oxide, retained ∼15% of the initial intensity before the removal. In the past, electron spin resonance signals of centers detected by SDR via defects situated at Si/SiO_2 interfaces disappeared after the removal of native oxide with dilute HF.[13,15,16] The fact that the peak intensity remained observable implies that Si-KU1 defects can exist both at Si/SiO_2 interfaces and bare or hydrogen-terminated Si surfaces. Leaving the sample in air at room temperature after the oxide removal leads to the formation of native surface oxide. Figure 2 shows clearly that the original intensity is regained after ∼10 days of native oxide formation in air.

Comparison of the Si-KU1 spectroscopic features with those previously published for silicon reveals that the

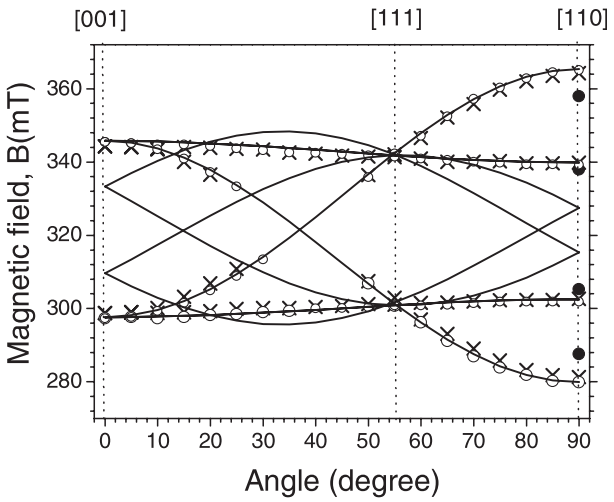

FIG. 4. Angular dependences of Si-KU1 line positions. Crosses (×) are positions of lines detected with native oxide on the surface, and open circles (○) are the line positions after chemical etching. Filled circles (•) are the line positions of the Si-SL1 spectrum for B‖[110] as in Fig. 2. Solid curves are the calculated angular dependences.

TABLE I. Principal values of $\boldsymbol{g}$ and $\boldsymbol{D}$ tensors. The principal axes labeled 1, 2, and 3 are parallel to [110], [$\bar{1}$10], and [001], respectively.

Spectrum spin S = 1	g_1	g_2	g_3 (±0.0004)	D_1	D_2	D_3 MHz (±2 MHz)	Fine structure splitting ΔB at B‖[110], mT	Ref.
Si-KU1 after etching by HNO_3 + HF	2.0060	2.0105	2.0080	±800	∓350	∓450	85.7	This work
Si-KU1 at native Si/SiO_2 interfaces	2.0040	2.0105	2.0080	±775	∓347	∓428	83.0	This work
Si-SL1 O + V center	2.0057	2.0102	2.0075	−657	307	350	70.26	14
Si-WL3 O + V in e-irradiated Si at 360–420 °C	2.0040	2.0100	2.0075	±719	∓334	∓385	77.0	11

Si-KU1 spectrum is similar to that reported for Si-SL1 EPR, which arises from photo-excited $S = 1$ triplet states of oxygen + vacancy complex.[14] This strongly implies that the Si-KU1 originates from an ensemble of $S = 1$ photo-excited centers situated at the Si surface or Si/SiO_2 interface. However, the fine-structure splitting between Si-KU1 and Si-SL1 is different as shown in Fig. 3. Here, SDR-EPR spectra are shown for the (100) Cz samples before and after boron ion implantation to produce Si-SL1 centers. The Si-KU1 spectrum disappeared after mechanical grinding of the sample surface and appeared again after chemical etching with solution having a HNO_3:HF ratio of 3:1. Thus, mechanical damage removes the Si-KU1-related defects. In addition, the Si-KU1 spectrum disappeared with annealing at temperatures above 400 °C. For a similar reason, the Si-KU1 spectrum was not observed for the samples with thermal oxides prepared at 800 °C and above.

The experimentally observed angular dependence of the line positions of the Si-KU1 spectrum is shown in Fig. 4. Here, excellent fitting (solid curves) was obtained with the Hamiltonian for spin $S = 1$ centers with $\boldsymbol{g}$ and $\boldsymbol{D}$ tensors having orthorhombic (C_{2v}) symmetry

$$H = \beta \boldsymbol{SgB} + \boldsymbol{SDS}. \quad (1)$$

The first term in Eq. (1) describes the electron Zeeman interaction, where β is the Bohr magnetron. The second term describes the fine structure resulting from the magnetic dipole–dipole interaction between the two electrons forming spin $S = 1$. $\boldsymbol{D}$ is a traceless tensor with principal values $D_1 + D_2 + D_3 = 0$, where the numbers 1, 2, and 3 represent the principal axes parallel to [110], [$\bar{1}$10], and [001], respectively. Values of the parameters g_1, g_2, g_3, D_1, D_2, and D_3 for the Si-KU1 spectrum determined by the fitting are listed in Table I. As can be seen in Fig. 1, the shapes of low-field and high-field lines are symmetric around the center of the spectrum. It shows that the line shape of the Si-KU1 spectrum is determined by the distribution of D parameters rather than by the g values that can be disturbed easily by random internal stress at the interface. More importantly, note that the solid curves in Fig. 4 were calculated for all six ⟨110⟩ equivalent orientations in a bulk silicon crystal. However, as can be seen in Fig. 4, only the two orientations of the [110] and [$\bar{1}$10] axes parallel to the Si wafer surface and Si/SiO_2 interface were detected. It shows that the observed spectrum arises from the defects localized at the sample surface and Si/SiO_2 interface.

The symmetry of the Si-KU1 spectrum is similar to that of the Si-SL1 spectrum of the excited triplet state of the oxygen + vacancy (O + V) complex[14] and to that of the Si-WL3 spectrum that is the modification of O + V centers produced by 1-MeV electron irradiation at higher temperatures (360–420 °C).[11] Moreover, several EPR spectra of spin $S = 1$ centers having orthorhombic symmetry were observed in neutron-irradiated[17] and helium-ion-implanted silicon.[18,19] However, the absolute values of parameters of these spectra are different from those of the Si-KU1 spectrum; i.e., Si-KU1 is the surface- and interface-related defects that have not been reported before.

The microscopic structure of the Si-KU1 centers can be conjectured according to the well-established Si-SL1 center involving oxygen and vacancy complexes.[14] Here, an oxygen atom localized around the substitutional position forms chemical bonds with two neighboring Si atoms. The two remaining dangling bonds of the silicon vacancy form the bonding and antibonding molecular orbitals oriented along any one of six equivalent ⟨110⟩ crystal axes.[14] In the excited triplet states, two electrons with parallel spins are localized in the bonding and antibonding orbitals. Therefore, our suggested model of the Si-KU1 center comprises molecular orbitals formed by two neighboring dangling bonds placed along two perpendicular [110] and [$\bar{1}$10] directions that lie parallel to the (100) plane because these are the only directions for which Si-KU1 spectra have been observed. Moreover, the Si-KU1 having orthorhombic symmetry suggests that it may be the photo-excited spin-triplet states of the $S = 1/2$ P_m center situated around Si/SiO_2 interfaces, which also has orthorhombic symmetry.[13] The intensities of both P_m (Ref. 13) and Si-KU1 SDR-EPR signals increase over several days during oxidation in air at room temperature.

In conclusion, a series of previously unreported, photo-excited spin-one ($S = 1$) electron paramagnetic resonance peaks labeled Si-KU1 has been detected for silicon wafers with and without native oxide layers on the surface. The series disappeared with heat treatments above 400 °C. The Si-KU1 spectrum has orthorhombic symmetry lying along two ⟨110⟩ orientations parallel to the Si/SiO_2 interface and bare silicon surface. A possible microscopic model of the defect responsible for the Si-KU1 spectrum was presented.

This work was supported in part by CREST-JST, in part by a Grant-in-Aid for Scientific Research and the Project for Developing Innovation Systems of MEXT, and in part by the JSPS Core-to-Core Program.

[1]P. M. Lenahan and M. A. Jupina, Colloids Surf. **45**, 191 (1990).
[2]Y. Nishi, Jpn. J. Appl. Phys., Part 1 **10**, 52 (1971).
[3]E. H. Poindexter, P. J. Caplan, B. E. Deal, and R. R. Razouk, J. Appl. Phys. **52**, 879 (1981).

[4]K. L. Brower, Semicond. Sci. Technol. **4**, 970 (1989).
[5]C. R. Helms and E. H. Pointdexter, Rep. Prog. Phys. **57**, 791 (1994).
[6]M. Jivanescu, A. Stesmans, and M. Zacharias, J. Appl. Phys. **104**, 103518 (2008).
[7]D. J. Lepine, Phys. Rev. B **6**, 436 (1972).
[8]R. L. Vranch, B. Henderson, and M. Pepper, Appl. Phys. Lett. **52**, 1161 (1988).
[9]L. S. Vlasenko, M. P. Vlasenko, V. N. Lomasov, and V. A. Khramtsov, Zh. Eksp. Teor. Fiz. **91**, 1037–1049 (1986) [Sov. Phys. JETP **64**, 612 (1986)].
[10]R. Laiho, L. S. Vlasenko, and M. P. Vlasenko, Mater. Sci. Forum **196–201**, 517 (1995).
[11]M. M. Afanasjev, R. Laiho, L. S. Vlasenko, and M. P. Vlasenko, Mater. Sci. Forum **258–263**, 559 (1997).
[12]L. S. Vlasenko, Solid State Phys. **41**, 697 (1999).
[13]T. Matsuoka, L. S. Vlasenko, M. P. Vlasenko, T. Sekiguchi, and K. M. Itoh, Appl. Phys. Lett. **100**, 152107 (2012).
[14]K. L. Brower, Phys. Rev. B **4**, 1968 (1971).
[15]H. Morishita, L. S. Vlasenko, H. Tanaka, K. Semba, K. Sawano, Y. Shiraki, M. Eto, and K. M. Itoh, Phys. Rev. B **80**, 205206 (2009).
[16]W. Akhtar, H. Morishita, K. Sawano, Y. Shiraki, L. S. Vlasenko, and K. M. Itoh, Phys. Rev. B **84**, 045204 (2011).
[17]Y.-H. Lee and J. W. Corbett, Phys. Rev. B **13**, 2653 (1976).
[18]Yu. V. Gorelkinskii, N. N. Nevinnyi, and S. S. Ajazbaev, Phys. Lett. A **110**, 157 (1985).
[19]Yu. V. Gorelkinskii, N. N. Nevinnyi, and S. S. Ajazbaev, Phys. Lett. A **125**, 354 (1987).